



Effect of activated carbon in distinguishing the electrochemical activity of hydroquinone and catechol at carbon paste electrode

H. Hammani^{1,2} · F. Laghrib¹ · S. Lahrach¹ · A. Farahi³ · M. Bakasse⁴ · A. Aboulkas² · M. A. El Mhammedi¹

Received: 23 December 2017 / Revised: 21 April 2018 / Accepted: 8 July 2018 / Published online: 17 July 2018
© Springer-Verlag GmbH Germany, part of Springer Nature 2018

Abstract

An activated carbon was prepared using physical activation from date stone. This activated carbon was characterized by SEM, XRD, and FT-IR. This composite was used as modifier of carbon paste electrode (AC/CPE) for electrochemical determination of catechol (CC) and hydroquinone (HQ) using cyclic voltammetry. The electrochemical experiments indicated that the modified electrodes can simultaneously determine HQ and CC at an oxidative and reductive peaks separation of about 125 and 120 mV, respectively. Furthermore, differential pulse voltammetry (DPV) of the sensing platform showed wide linear responses in the presence of $5.0 \times 10^{-5} \text{ mol L}^{-1}$ CC with the limit of detection ($S/N=3$) of $7.1 \times 10^{-8} \text{ mol L}^{-1}$. At the same time, the oxidation peak current of CC was linear to its concentration with the limit of detection ($S/N=3$) of $5.23 \times 10^{-8} \text{ mol L}^{-1}$ in the presence of $1.0 \times 10^{-4} \text{ mol L}^{-1}$ HQ.

Keywords Sensors · Materials preparations · Electrochemical characterizations · Catalysis

Introduction

Phenolic compounds and its substitute are important organic intermediates for the products of industrial raw and synthetic in cosmetic, pharmaceutical, tanning, and pesticide industries, etc. [1–4], for example, dihydroxybenzene compounds such as catechol (CC, 1,2-benzenediol) and hydroquinone (HQ, 1,4-benzenediol). Unfortunately, these two isomers are broadly distributed in soil and aquatic environment and are difficult to be degraded due to their high toxicity and high stability in the ecological environment [5–7]. It is highly toxic to human health even at very low concentrations [8], which are

considered as environmental pollutants by the US Environmental Protection Agency (EPA) and the European Union (EU) [9]. Moreover, CC and HQ usually coexist in the environmental samples and have similar structures and properties, which make it difficult to determine them simultaneously. Therefore, the development of a sensitive, simple, and rapid method for simultaneous determination of HQ and CC has become the most important study.

Up to now, many instrumental methods such as chromatography [10], chemiluminescence [11, 12], and spectrophotometry [13] have been commonly employed for quantification of CC and HQ. In fact, these techniques require expensive, complicated instruments and time consuming procedure. However, the electrochemical methods offer the practical advantages including easy operation, satisfactory sensitivity, and low cost of instrument [14–21]. The simultaneous determination of the two dihydroxybenzene isomers CC and HQ represents a serious problem, which arises from the adjacent potentials in the direct oxidation and reduction at most unmodified electrode surfaces. Therefore, it is very important to develop novel materials with excellent conductivity and catalytic activity for the simultaneous determination of CC and HQ.

Activated carbon (AC) is a carbonaceous material, and it is highly porous over a broad range of pore sizes and various functional groups on the surface [22, 23]. Due to their good chemical stability, large aspect ratio, excellent electrical

✉ M. A. El Mhammedi
elmhammedi@yahoo.fr

¹ Laboratoire de Chimie et Modélisation Mathématique (LCMM), Faculté Polydisciplinaire, Univ. Hassan 1^{er}, BP 145, 25000 Khourigba, Morocco

² Laboratoire des procédés chimiques et matériaux appliqués (LPCMA), Faculté Polydisciplinaire, Univ. Sultan Moulay Slimane, BP 592, 23000 Béni Mellal, Morocco

³ Equipe de Catalyse et Environnement, Faculté de Sciences, Univ. Ibn Zohr, BP 8106 Cité Dakhla, Agadir, Morocco

⁴ Equipe d'Analyse des Micropolluants Organiques, Faculté de Sciences, Univ. Chouaib Doukkali, El Jadida, Morocco

conductivity, and being cost effective [24–27], AC was widely used in the development of high-performance electrochemical sensors [28]. The price of commercial activated carbon varies between 0.8 and 10 €/kg [29]. However, because the commercial production of activated carbon is not cost effective and together with the fact that the regeneration of used activated carbon is extremely difficult, much attention has been given to synthesizing amorphous activated carbon from renewable sources [30]. Many researchers turn their attention from fossil fuels to cheaper biomass, which is viewed as a veritable way to make full use of agricultural/industrial wastes and reduce carbon emission [31–33].

The novelty of this work is the simultaneous determination of the catechol and hydroquinone using an AC. This material having the advantages of very low cost and facilitates the charge transfer, which can enhance the electrocatalytic performance and anti-interference proprieties of the modified electrode.

In this study, we presented a simple and general method to prepare activated carbon from date stone through physical activation. The result was demonstrated to be an effective material for the fabrication of electrochemically modified paste carbon electrode (AC/CPE). The performance of the fabricated electrode (AC/CPE) and their catalytic effect on HQ and CC behaviors were investigated using cyclic voltammetry (CV). Moreover, the fabricated AC/CPE was successfully applied to the simultaneous detection of HQ and CC by differential pulse voltammetry (DPV) with good sensitivity, wide linear range, and low limit of detection.

Experimental

Reagents

All reagents employed were of analytical grade and were used without further purification. Hydroquinone (HQ) and catechol (CC), dibasic potassium phosphate, and potassium dihydrogen phosphate were obtained from Sigma-Aldrich. Its stock solution was prepared with distilled water. Phosphate buffer solutions were prepared by mixing the stock solutions of 0.1 mol L⁻¹ K₂HPO₄ and 0.1 mol L⁻¹ KH₂PO₄ at different ratios to adjust the pH value. Carbon graphite powder (particle size < 100 μm) used for constructing electrodes was supplied from Carbone Lorraine (Lorraine, France; ref. 9900).

Apparatus

The electrochemical experiments, including cyclic voltammetry (CV) and differential pulse voltammetry (DPV), were performed with an eDAQ recorder/potentiostat EA163 controlled by the eDAQChem data acquisition software, with

a three electrode system. The working electrode was unmodified carbon paste or that modified by activated carbon (AC/CPE) with cavity geometric surface of 0.1256 cm². Reference electrode and counter electrode used were Ag/AgCl/saturated KCl and platinum, respectively. pH measurements were carried out using a pH-meter sensION™ (pH 31), with a combined pH glass electrode calibrated against standard phosphate buffer solutions.

The activated carbon was characterized by X-ray diffraction (D 2-PHASER of BRUKER-AXS, Cu-radiation, λKα₁ = 1.54060 Å and λKα₂ = 1.54439 Å) performed at room temperature. The external surface of the activated carbon was examined by a scanning electron microscope VEGA3 TESCAN. Fourier Transform Infrared (FT-IR) spectroscopy (FTIR-2000, Perkin Elmer) was used also to evaluate the chemical structure properties. The infrared spectrum was collected in a range of 4000–400 cm⁻¹.

Preparation of activated carbon modified carbon paste electrode

The activated carbon was prepared according to the method reported in the literature [34]. Briefly, activated carbons were prepared from date stones by pyrolysis under nitrogen flow and activation under water vapor. Moreover, the carbon paste mixture was prepared by hand mixing of graphite powder and an appropriate amount of activated carbon to form a mixture well homogenized [34, 35].

Results and discussion

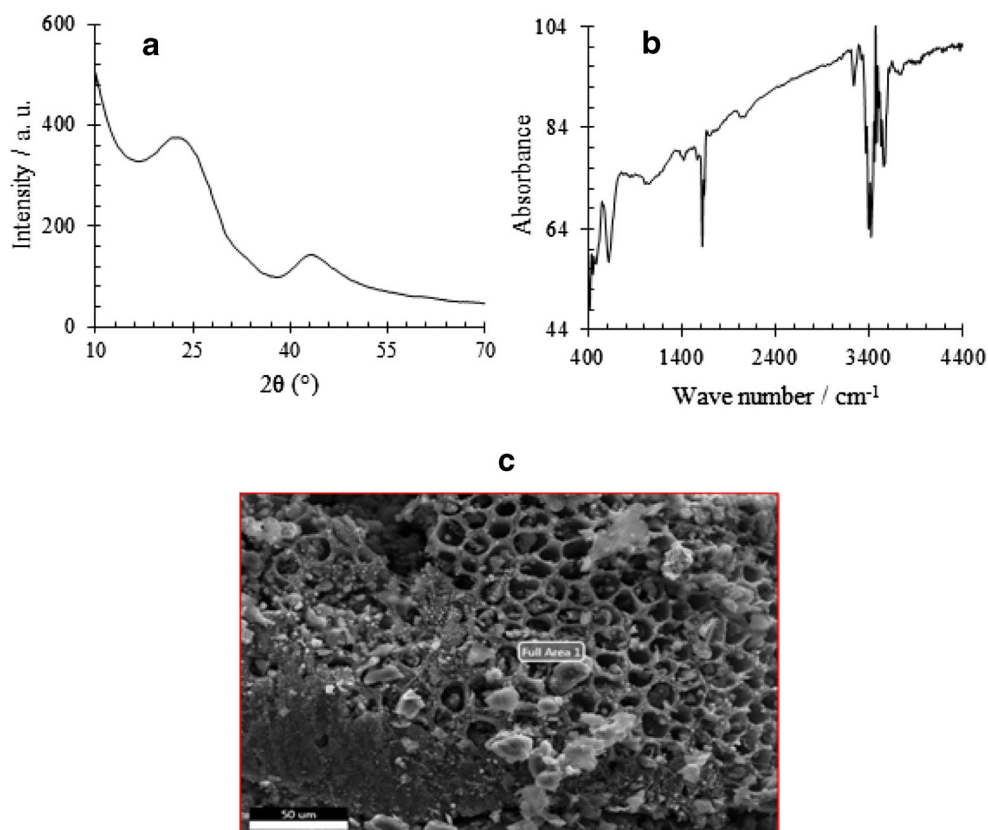
Characterization of the activated carbon

X-ray diffraction patterns for activated carbon were shown in Fig. 1a. The positions of the peaks due to *d*₀₀₂ and *d*₁₀₀ reflections are attributed to 2θ = 23.5° and 43.5°, respectively [36]. These diffraction peaks are evidence that the samples have an amorphous structure.

FT-IR was used to determine the functional groups involved in activated carbon. In the FT-IR spectra (Fig. 1b), the presence of –OH group stretching at wave number of 3500 cm⁻¹ (stretching vibration) with low signal was indicated. Similarly, at wave number of 2924 cm⁻¹, it was attributed to C–H interaction with the surface of the carbon [37], with moderate intensity. Then, the wave numbers of 1645 cm⁻¹–1678 cm⁻¹ showed the C=C bonds of an alkene compound type, while 1516 cm⁻¹–1541 cm⁻¹ showed the C=C bonds of the aromatic ring compound type; this is supported by the presence of C–O at wave number of 1112 cm⁻¹ [38].

Scanning electron microscope (SEM) picture of activated carbon is shown in Fig. 1c. The picture shows the highly porous characteristics of activated carbon with full of cavities.

Fig. 1 **a** X-ray diffraction (XRD). **b** Infrared spectra (IR). **c** SEM-EDX of activated carbon



The porous surface morphology of the prepared carbon is a positive point for adsorption of hydroquinone and catechol.

Effect of activated carbon on the separation peak potential of HQ and CC

Figure 2a, b displays the individual electrochemical behaviors of HQ and CC at the CPE and AC/CPE in 0.1 M PBS (pH 7.0), respectively. From Fig. 2a, it can be observed that at AC/CPE, the potential differences between anodic and cathodic peaks of HQ were determined to be 0.233 and -0.037 V, respectively. After the CPE modified with AC, the peak potential separation (ΔE_p) decreased from 0.49 to 0.27 V. For CC (Fig. 2b), at CPE, the abroad anodic and cathodic peak potentials of CC appear at about 0.393 and 0.016 V, respectively. While at AC/CPE, the anodic and cathodic peaks appear at 0.312 and 0.054 V, respectively, and the ΔE_p is extensively narrowed to 119 mV. The above results further confirm that the electrochemical reversibility of CC at the AC/CPE can be improved, similar to the observation in the case of HQ at the AC/CPE. It is evident that the AC could be an effective electrocatalyst for the redox reaction of dihydroxybenzene isomers.

The cyclic voltammograms of a mixture containing HQ and CC (1.0×10^{-3} mol L $^{-1}$) in PBS (pH 7.0) at CPE and AC/CPE are shown in Fig. 2c. At CPE, a large broad peak

centered at +0.314 V is observed for the oxidation reaction, while a narrower peak centered at 0.022 V is observed for the reduction reaction. These behaviors showed that the oxidation and reduction peaks of HQ and CC were characterized by the overlapping peaks, and it was impossible to separate these two compounds easily at the CPE. Also, the peak potential separation ($\Delta E_p = E_{pa} - E_{pc}$) of 292 mV indicates the irreversibility of the reactions. On the other hand, at AC/CPE, two pairs of well-defined peaks are apparent. The peaks at +0.022 and +0.147 V correspond to the oxidation of HQ and CC, respectively, and the reduction peaks are observed at -0.016 V (HQ) and +0.104 V (CC), with the values of $\Delta E_p = 38$ mV for HQ and $\Delta E_p = 43$ mV for CC. Additionally, a separation of 125 and 120 mV between the oxidation and reduction peaks, respectively, of HQ and CC is large enough for the simultaneous determination of the dihydroxybenzene isomers. The AC/CPE electrode exhibited an efficient electrocatalytic oxidation of HQ compared to CC (peak shift), due to high adsorption of the proposed modifier toward the molecules containing more than one groupment “OH.” The variation of the adsorption capacity as a function of the “OH” position serves to promote the separation of the HQ and CC peaks. From the obtained results, it is found that the HQ adsorbs better than the CC. Consequently, the best adsorption capacity was observed for the molecule with “para” position compared to the ortho isomers. As well as the difference between the

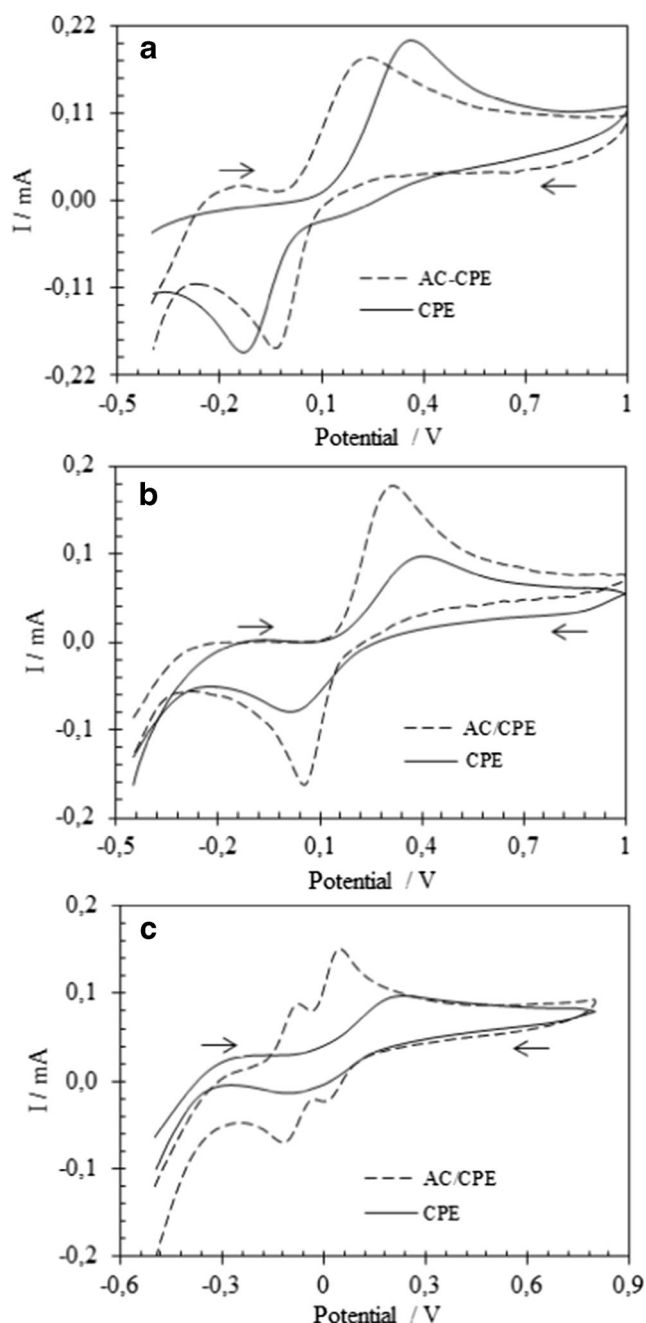


Fig. 2 a, b, and c are CVs of $1.0 \times 10^{-3} \text{ mol L}^{-1}$ HQ, $1.0 \times 10^{-3} \text{ mol L}^{-1}$ CC, and mixture of $1.0 \times 10^{-3} \text{ mol L}^{-1}$ HQ and $1.0 \times 10^{-3} \text{ mol L}^{-1}$ CC in 0.1 mol L^{-1} PBS (pH 7.0) at CPE and AC/CPE at 50 mV s^{-1} , respectively

oxidation potentials facilitated the sensitive and accurate detection of the two compounds [39–41].

The excellent performance of AC/CPE may attribute to the following reasons. Firstly, the hydroxyl, carboxyl, and lactonic groups in activated carbon could interact with the hydroxyl groups in two isomers (CC and HQ) via H-bonding. Secondly, in the PBS of pH 7.0, the negatively charged AC ($\text{pH}_{\text{zpc}} = 7.6$) could also interact with the positively charged HQ ($\text{pK}_a 9.96$) and CC ($\text{pK}_a 9.48$) through the favorable electrostatic

attraction. These interactions may help to lower the activation energy of the redox reactions required. The overpotential of reactions was therefore decreased. Thirdly, the two isomers can be enriched on AC/CPE due to the large specific surface area of the AC.

Optimization of parameters

Effect of the mass ratio of AC

In order to obtain a better electrochemical performance of modified paste carbon electrode (AC/CPE) for the simultaneous detection of HQ and CC, the mass ratio of AC used in the fabrication of the modified electrode was investigated by CV. From Fig. 3, the modified electrodes fabricated with different mass ratios of AC behaved differently on the detection. When the mass ratio of AC was 2%, the resulting modified electrode exhibited the largest peak current, while the oxidation peak of HQ and CC could be completely separated. Thus, the optimum mass ratio of AC was selected as 2%.

Effect of solution pH

The electrochemical oxidation of hydroxyl aromatic compounds always involves proton transfer to form quinone [42]. So, to obtain the best electrochemical response of HQ and CC at the AC/CPE, the effect of the solution pH on the electrochemical responses was also investigated by the CV in 0.1 mol L^{-1} buffer phosphate solution, with a pH range of 5–8.5. As can be seen in Fig. 4, the anodic peak potentials of HQ and CC shifted negatively with the increase of pH from 5 to 8.5, revealing the participation of protons in the present electrochemical redox process [43]. The linear relationship of the formal potential of HQ and CC with pH can be expressed as the following equations (Eq. (1) and (2)):

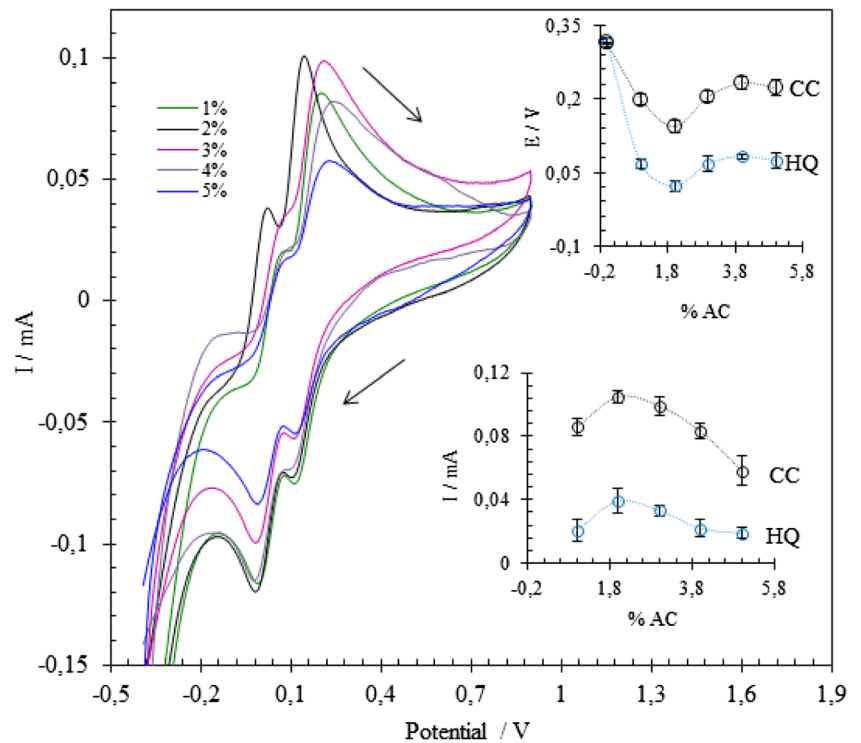
$$\text{HQ} : E_{\text{pa}} (\text{V}) = 0.5594 - 0.0574 \text{ pH} \quad (R^2 = 0.9715) \quad (1)$$

$$\text{CC} : E_{\text{pa}} (\text{V}) = 0.3187 - 0.0420 \text{ pH} \quad (R^2 = 0.9917) \quad (2)$$

The slopes values of the two equations closed well with the theory value of 59 mV/pH that deduced from the Nernst equation ($dE_{\text{p}}/d\text{pH} = 2.303 \text{ mRT}/nF$, m and n are protons and electrons numbers). Based on these results, the redox reaction of HQ (or CC) at AC/CPE should be a two electron and two proton processes [44, 45]. Therefore, the probable reactions of HQ and CC on AC/CPE are described as Schema 1.

Figure 4 also shows that the oxidation peak current of HQ and CC increased with increasing the pH value until 7.0 and then decreased when the pH further increased. For the detection of HQ and CC simultaneously, pH 7.0 was selected as an optimal value of pH.

Fig. 3 CVs of AC/CPE with the mass ratios of AC at 1, 2, 3, 4, and 5% in 0.1 mol L⁻¹ PBS (pH 7.0) containing 1.0 × 10⁻³ mol L⁻¹ HQ and 1.0 × 10⁻³ mol L⁻¹ CC; plots of variation of *I*_a and *E*_a with mass ratios of AC

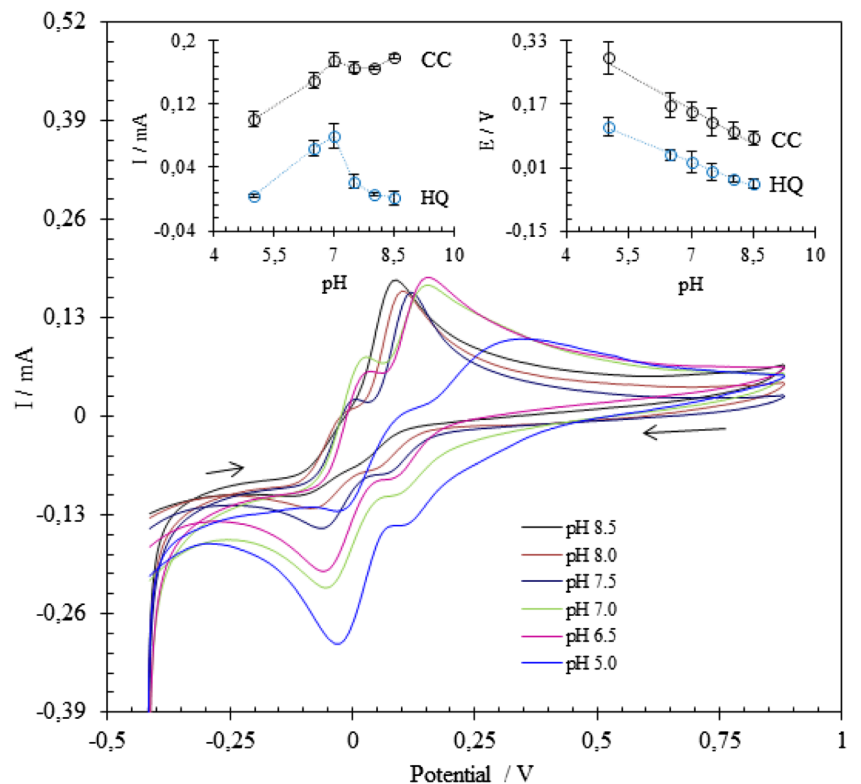


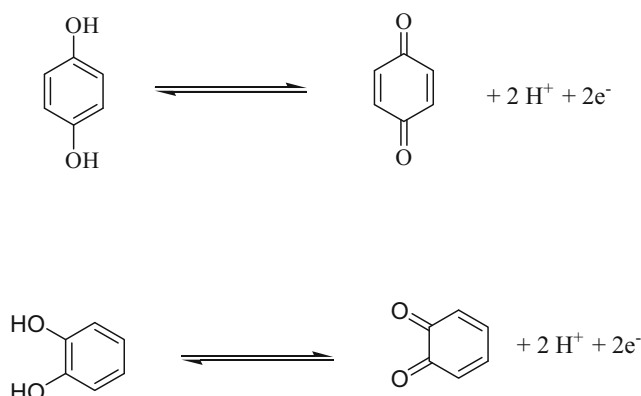
Effect of scan rate

The effect of scan rate on the redox of two isomers HQ and CC were investigated on the AC/CPE using CV. Figure 5

showed the CV plots with different scan rates (30–400 mV s⁻¹) in 1.0 × 10⁻³ mol L⁻¹ HQ and CC. The oxidation peaks current vs. scan rate for the HQ and CC which exhibited the linearity with the linear regression equation *I*_{pa} (μA) =

Fig. 4 CVs at AC/CPE in 0.1 mol L⁻¹ PBS with different pH containing 1.0 × 10⁻³ mol L⁻¹ HQ and 1.0 × 10⁻³ mol L⁻¹ CC; plot of *E*_a CC and *E*_a HQ vs. pH value; plot of *I*_a CC and *I*_a HQ vs. pH value





Schema 1 Redox reaction of HQ and CC

$0.114 \nu \mu\text{A}/\text{mVs}^{-1} + 3.63 \mu\text{A}$ ($R^2 = 0.9966$) for HQ and I_{pa} (μA) = $0.133 \nu \mu\text{A}/\text{mVs}^{-1} + 6.15 \mu\text{A}$ ($R^2 = 0.9959$) for CC. From the slopes (0.8606 and 0.8613) found from the graph of log sweep rate (ν) versus the Log of anodic peak current (Log I_{pa}) for HQ and CC is nearly to the theoretically obtained value of 1.0 for an adsorption controlled electrode process [46, 47]. This study indicates that the electrocatalytic behavior of HQ and CC at the surface of AC/CPE was controlled by the adsorption controlled electrochemical process [48].

Simultaneous determination of HQ and CC

Differential pulse voltammetry technique (DPV) has been established to be very sensitive in the detection of micromolar amounts of chemical species compared with cyclic voltammetry. The effect of the chemical and DPV parameters on the

response of the electrodes has been studied by means of seven factors. According to our experience, the optimal combination of chemical and DPV parameters chosen for these studies was as follows: accumulation time = 60 s, pH = 7, mass ratio of AC = 2%, step weight = 150 ms, step height = 5 mV, pulse weight = 50 ms, and step height = 80 mV.

The selective determination of HQ and CC at AC/CPE was studied by increasing the concentration of one isomer while keeping the concentration of the other isomer constant. Figure 6a shows that the DPV signals of CC oxidation increased remarkably with the increase of CC concentration, and the coexisted HQ had no effect on the detection of CC. As shown in the insert of Fig. 6a, the increase of I_{pa} fits the linear equation of I_{pa} (μA) = $0.2457 [\text{CC}]$ ($\mu\text{mol L}^{-1}$) + 16.07 ($R^2 = 0.9965$) when the concentration of CC increases from 1.0×10^{-6} to $1.0 \times 10^{-3} \text{ mol L}^{-1}$. The AC/CP exhibits good limit of detection (LOD) and limit of quantification (LOQ) for CC using Eq. (3) and (4) [49, 50] and found to be $1.83 \times 10^{-8} \text{ mol L}^{-1}$ and $5.5 \times 10^{-8} \text{ mol L}^{-1}$, respectively.

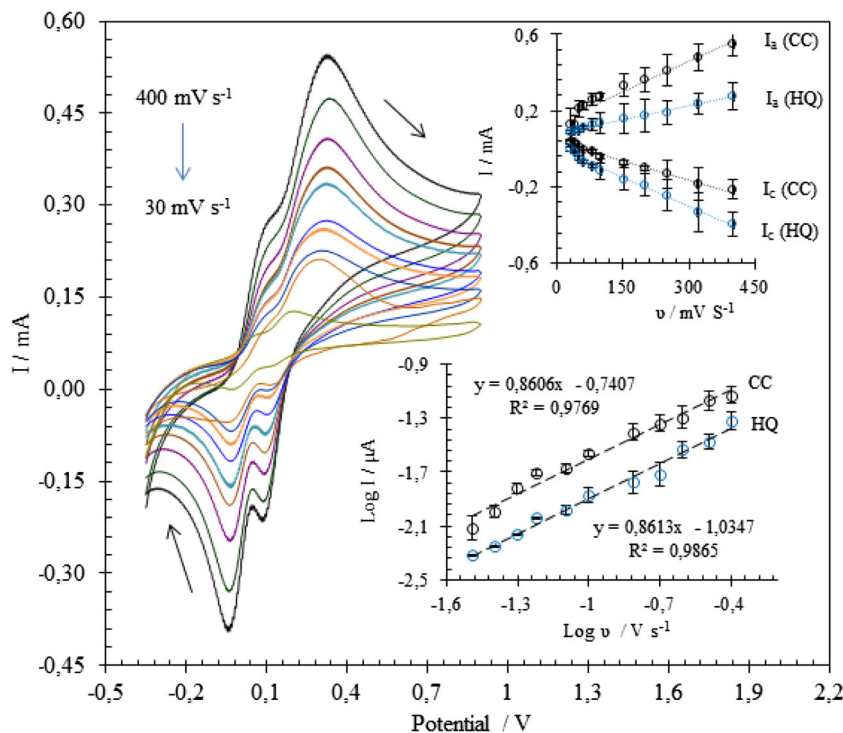
$$\text{LOD} = 3S/M \quad (3)$$

$$\text{LOQ} = 10S/M \quad (4)$$

where, S is the standard deviation and M is the slope.

Similarly, as shown in Fig. 6b, in the coexistence of CC, the linear range of HQ was from 1.0×10^{-7} to $1.0 \times 10^{-3} \text{ mol L}^{-1}$ with a regression equation of I_{pa} (μA) = $0.1907[\text{HQ}]$ ($\mu\text{mol L}^{-1}$) + 8.945 ($R^2 = 0.9943$). The calculated LOD and LOQ are $7.1 \times 10^{-8} \text{ mol L}^{-1}$ and $2.36 \times 10^{-7} \text{ mol L}^{-1}$,

Fig. 5 CVs of a mixture of $1.0 \times 10^{-3} \text{ mol L}^{-1}$ HQ and CC in 0.1 mol L^{-1} PBS on AC/CPE at different scan rates (30, 40, 50, 60, 80, 100, 153, 200, 250, 320, and 400 mV s^{-1}); plot I vs. scan rate; plot Log I_a vs. Log ν



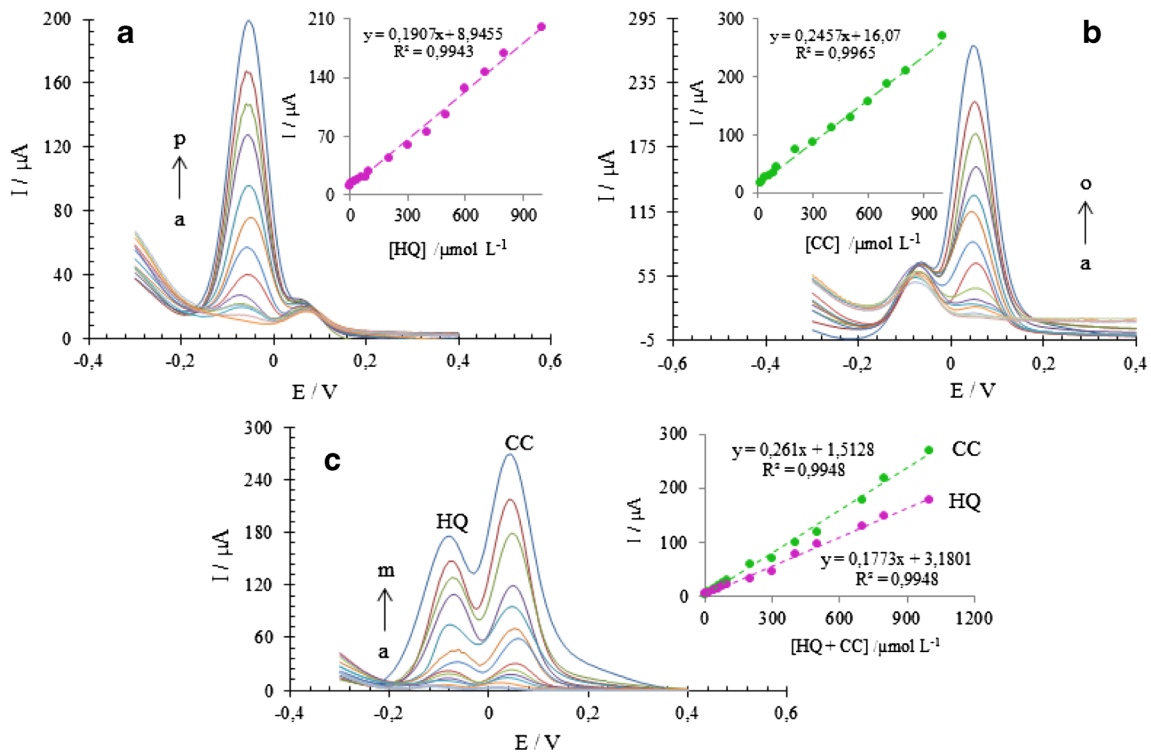


Fig. 6 DPVs of AC/CPE in 0.1 mol L⁻¹ PBS (pH 7.0) containing **a** various concentrations of HQ (a–p 1.0 × 10⁻⁷ to 1.0 × 10⁻³ mol L⁻¹) in the presence of 5.0 × 10⁻⁵ mol L⁻¹ CC, **b** various concentrations of CC (a–o 1.0 × 10⁻⁶ to 1.0 × 10⁻³ mol L⁻¹) in the presence of 1.0 × 10⁻⁴ mol L⁻¹ HQ, and **c** various concentrations of HQ and CC (a–m 1.0 × 10⁻⁶ to 1.0 × 10⁻³ mol L⁻¹). The inserts show the relationships between the peak currents and target concentrations

respectively. The above results indicate that the oxidation reactions of HQ and CC at AC/CPE take place independently.

The simultaneous determination of HQ and CC at AC/CPE was further studied by synchronously changing the concentration of HQ and CC in their binary mixture. The results are shown in Fig. 6c. The oxidation peak currents of HQ and CC were linearly correlated with their concentrations. The regression equations for CC and HQ were $I_{pa} (\mu A) = 0.261 [CC] (\mu mol L^{-1}) + 1.5128$ ($R^2 = 0.9948$) and $I_{pa} (\mu A) = 0.1773 [HQ] (\mu mol L^{-1}) + 3.1801$ ($R^2 = 0.9948$), and the limit of

detection was estimated to be 5.23×10^{-8} mol L⁻¹ and 7.7×10^{-8} mol L⁻¹, respectively. These values are, respectively, in accordance with those obtained in their selective detection. It is confirmed that the fabricated AC/CPE is suitable for the simultaneous detection of HQ and CC in mixed systems.

A comparison of the proposed electrode AC/CPE with other electrodes for HQ and CC detection is listed in Table 1. Our proposed method achieved lower limits of detection, wider linear concentration ranges, and larger separation anodic potential (ΔE_p) value toward the simultaneous

Table 1 Comparison of the fabricated AC/CPE with other reported modified electrodes for the detection of HQ and CC

Modified material	Linear range (10 ⁻⁶ mol L ⁻¹)		LOD (10 ⁻⁶ mol L ⁻¹)		ΔE_p (mV)	Reference
	HQ	CC	HQ	CC		
Chi/GR	1–300	1–400	0.75	0.75	96	3
GMC	2–50	2–70	0.37	0.31	130	8
PEDOT/GO	2.5–200	2–400	1.60	1.60	100	48
PDA/RGO	1–250	1–230	0.62	0.74	103	51
Nafion-FEPA-CNP/GR	0.3–90	0.6–100	0.157	0.272	105	52
Poly(glutamic acid)/GCE	5–80	1–80	1.0	0.8	102	53
AC/CPE	1–1000	0.1–1000	0.07	0.05	125	This work

Chi-GR chitosan-graphene, *GMC* graphitic mesoporous carbon, *PEDOT-GO* poly(3,4-ethylenedioxy-thiophene)-graphene oxide, *PDA-RGO* polydopamine-reduced graphene oxide, *Nafion-FEPA-CNP-GR* Nafion-(4-ferrocenylethyne) phenylamine-carbon nanoparticles-graphene, *Poly(glutamic acid)/GCE* poly(glutamic acid) modified glassy carbon electrode

Table 2 Influences of coexisting substances on the detection of 1.0×10^{-5} mol L⁻¹ HQ and CC

Interfering	Current ratios (%) ^a		Potential ratios (%) ^b	
	HQ	CC	HQ	CC
Na ⁺	-3.80 ± 0.12	-3.75 ± 0.65	-1.01 ± 0.85	-1.23 ± 0.74
Ni ²⁺	-1.19 ± 0.02	-0.22 ± 0.04	-0.82 ± 0.15	-0.43 ± 0.31
Zn ²⁺	+0.03 ± 0.48	-3.07 ± 0.99	+0.54 ± 1.12	+0.36 ± 0.22
Cd ²⁺	+0.55 ± 0.18	+0.46 ± 0.18	+1.12 ± 0.52	+1.89 ± 0.63
Ag ⁺	+1.61 ± 1.06	+0.41 ± 0.28	-2.13 ± 0.98	-3.11 ± 1.12
Al ³⁺	-0.28 ± 0.02	-3.38 ± 0.42	-0.15 ± 1.12	-1.23 ± 1.26
Mg ²⁺	-0.062 ± 0.17	+1.01 ± 0.85	+0.92 ± 0.06	+0.13 ± 0.14
Pb ²⁺	+0.34 ± 0.04	-1.46 ± 0.04	+1.16 ± 0.08	-0.65 ± 1.12
Co ²⁺	-1.64 ± 0.02	-1.56 ± 0.05	+1.98 ± 0.94	+2.29 ± 1.26
Fe ²⁺	+4.12 ± 1.63	+3.92 ± 2.16	-2.19 ± 0.05	-3.12 ± 2.65

^a Ratio of currents for mixtures of substance and HQ and CC compared with HQ and CC only

^b Ratio of potential for mixtures of substance and HQ and CC compared with HQ and CC only

determination of HQ and CC, which is superior to the reported in references [3, 8, 48, 51–53].

Interference of coexisting substances

The influence of various substances as compounds potentially interfering with the determination of HQ and CC was studied under optimum conditions. For this fact, the interferences of some common metal ions were evaluated. Experimental results which show the effect of some common metal ions including Na⁺, Ni²⁺, Zn²⁺, Cd²⁺, Ag⁺, Al³⁺, Mg²⁺, Pb²⁺, Co²⁺, and Fe²⁺ (each of 1.0×10^{-4} mol L⁻¹) on the peak potential and intensity of 1.0×10^{-5} mol L⁻¹ HQ and 1.0×10^{-5} mol L⁻¹ CC were represented in Table 2. The variation in current and potential peak caused by the interference metal ions was less than 5%, which proved an excellent selectivity of AC/CPE. Additionally, for the common interference in biological samples, 5.0×10^{-5} mol L⁻¹ of 4-nitrophenol, phenol, paracetamol, and dopamine were investigated in the presence of 5.0×10^{-5} mol L⁻¹ HQ and CC. The use of the AC/CPE for the simultaneous determination was demonstrated by the clean separation of the potential peaks compared with CPE (Fig. 7). These results demonstrated that the AC-modified electrode exhibited excellent selectivity for determination of CC and HQ without interference of other coexisting substances.

Stability and reproducibility of the AC/CPE

The stability and reproducibility of AC/CPE were also investigated by DPV and the modified electrodes exhibited nice properties in these two aspects. When the AC/CPE was stored at room temperature for about 1 month, the peak currents and

peak potential of HQ and CC decreased merely 5%, indicating the high stability of AC/CPE (Fig. 8a). In addition, under the optimized conditions, the reproducibility was investigated comparing the peak currents and peak potential of the same concentration of HQ and CC (Fig. 8b). The relative standard deviations (RSDs) were less to 4%, which obtained for eight measurements in a solution of 1.0×10^{-5} mol L⁻¹ CC and 1.0×10^{-5} mol L⁻¹ HQ.

Analytical application

In order to check the applicability and validity of the proposed method, the AC/CPE was applied for the simultaneous determination of HQ and CC in local tap water samples. Typically, the sample was prepared by adding 0.1 mol L⁻¹ PBS (pH 7) to

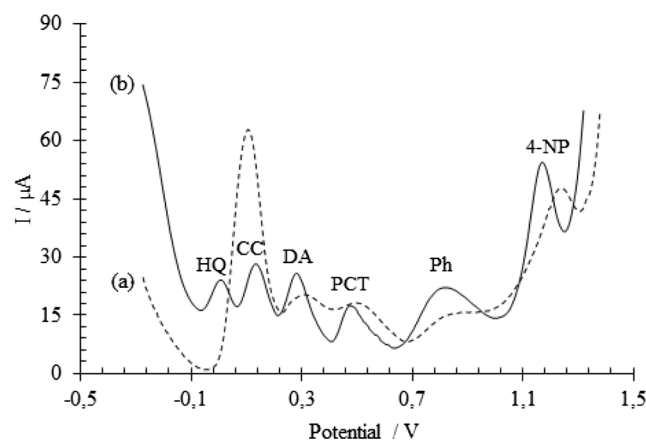


Fig. 7 DPV curves after exposure to a solution containing 5.0×10^{-5} mol L⁻¹ 4-nitrophenol (4-NP), phenol (Ph), paracetamol (PCT), dopamine (DA), hydroquinone (HQ) and catechol (CC) at CPE (a), and AC/CPE (b)

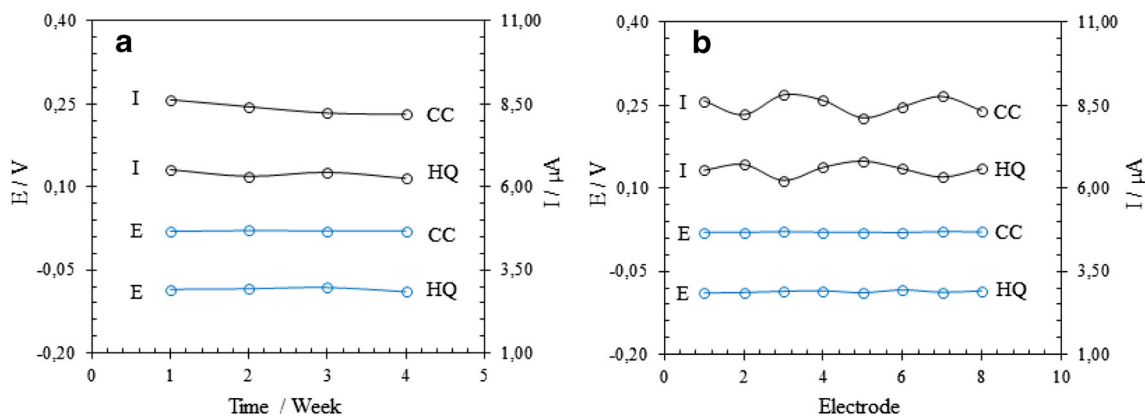


Fig. 8 The stability (a) and reproducibility (b) of AC/CPE with repetitive measurements of DPV response for 1.0×10^{-5} mol L⁻¹ CC and 1.0×10^{-5} mol L⁻¹ HQ in 0.1 mol L⁻¹ PBS with pH 7.0

tap water and then spiked with appropriate amounts of CC and HQ. The electroanalytical curves were recorded using differential pulse voltammetry.

The results demonstrated that no analytes could be detected in the real samples, meaning that two isomers HQ and CC contents were below than the limits of detection. Then, the amount of hydroquinone in the presence of catechol, as well as catechol in the presence of hydroquinone in local tap water samples, was calculated from the calibration method using differential pulse voltammetry and the results are summarized in Table 3. The recoveries were found in the range from 95.50 to 97.85% for HQ and from 95.25 to 98.60% for CC, with the RSDs (below 5%). The obtained recovery results indicate that AC/CPE modified electrode can be successfully used for the determination of the concentration of two dihydroxybenzene isomers in real tap water samples.

Conclusion

In this work, a facile, effective and highly sensitive electrochemical method is devoted based on the activated carbon for the simultaneous and quantitative detection of HQ and CC. Therefore, due to the excellent electrocatalytic activity of AC, it showed two well-defined voltammetric peaks with greatly

enhanced peak currents compared to that at bare CPE, which provided high sensitivity and good reversibility for the oxidation of HQ and CC. After the optimization of the experimental conditions, the measurable concentration ranges of HQ and CC using DPV at AC/CPE are expanded remarkably with lower limits of detection compared to previously reported electrochemical sensors. Additionally, the proposed modified electrode was applicable to determine HQ and CC in tap water with satisfying results. All the results showed that the proposed method is simple, low cost, and effective, which provides for the simultaneous detection of two diphenol isomers.

Acknowledgements The research described in this article has been funded wholly by the university Hassan I, Morocco.

References

- Du H, Ye J, Zhang J, Huang X, Yu C (2011) A voltammetric sensor based on graphene-modified electrode for simultaneous determination of catechol and hydroquinone. *J Electroanal Chem* 650:209–213
- Blaut M, Braune A, Wunderlich S, Sauer P, Schneider H, Glatt H (2006) Mutagenicity of arbutin in mammalian cells after activation by human intestinal bacteria. *Food Chem Toxicol* 44:1940–1947
- Yin H, Zhang Q, Zhou Y, Ma Q, Liu T, Zhu L, Ai S (2011) Electrochemical behavior of catechol, resorcinol and hydroquinone at graphene–chitosan composite film modified glassy carbon electrode and their simultaneous determination in water samples. *Electrochim Acta* 56:2748–2753
- Khodaei MM, Alizadeh A, Pakravan N (2008) Polyfunctional tetrazolic thioethers through electro-oxidative/Michael-type sequential reactions of 1,2- and 1,4- dihydroxybenzenes with 1-phenyl-5-mercaptotetrazole. *J Org Chem* 73:2527–2532
- Jagetia GC, Aruna R (1997) Hydroquinone increases the frequency of micronuclei in a dose-dependent manner in mouse bone marrow. *Toxicol Lett* 93:205–213
- Taysse L, Troutaud D, Khan NA, Deschaux P (1995) Structure-activity relationship of phenolic compounds (phenol, pyrocatechol and hydroquinone) on natural lymphocytotoxicity of carp (*Cyprinus carpio*). *Toxicology* 98:207–214
- Hirakawa K, Oikawa S, Hiraku Y, Hirokawa I, Kawanishi S (2002) Catechol and hydroquinone have different redox properties

Table 3 Obtained results for the determination of hydroquinone and catechol in tap water

Added (mol L ⁻¹) × 10 ⁻⁵	Found (mol L ⁻¹) × 10 ⁻⁵		Recovery (%)	
	HQ	CC	HQ	CC
0	<DL	<DL	–	–
8	7.64	7.62	95.50 ± 1.04	95.25 ± 0.92
10	9.73	9.86	97.30 ± 1.26	98.60 ± 2.07
20	19.57	19.63	97.85 ± 2.12	98.15 ± 2.96

- responsible for their differential DNA-damaging ability. *Chem Res Toxicol* 15:76–82
8. Yuan X, Yuan D, Zeng F, Zou W, Tzorbatozoglou F, Tsiakaras P, Wang Y (2013) Preparation of graphitic mesoporous carbon for the simultaneous detection of hydroquinone and catechol. *Appl Catal B Environ* 129:367–374
 9. Ahammad AJS, Sarker S, Rahman MA, Lee JJ (2010) Simultaneous determination of hydroquinone and catechol at an activated glassy carbon electrode. *Electroanalysis* 22:694–700
 10. Asan A, Isildak I (2003) Determination of major phenolic compounds in water by reversed-phase liquid chromatography after pre-column derivatization with benzoyl chloride. *J Chromatogr A* 988:145–149
 11. Li SF, Li XZ, Xu J, Wei XW (2008) Flow-injection chemiluminescence determination of polyphenols using luminol–NaIO₄–gold nanoparticles system. *Talanta* 75:32–37
 12. Cui H, Zhang QL, Myint A, Ge XW, Liu LJ (2006) Chemiluminescence of cerium(IV)–rhodamine 6G–phenolic compound system. *J Photochem Photobiol A Chem* 181:238–245
 13. Nagaraja P, Vasantha RA, Sunitha KR (2001) A sensitive and selective spectrophotometric estimation of catechol derivatives in pharmaceutical preparations. *Talanta* 55:1039–1046
 14. Unnikrishnan B, Ru PL, Chen SM (2012) Electrochemically synthesized Pt–MnO₂ composite particles for simultaneous determination of catechol and hydroquinone. *Sensors Actuators B Chem* 169:235–242
 15. Li DW, Li YT, Song W, Long YT (2010) Simultaneous determination of dihydroxybenzene isomers using disposable screen-printed electrode modified by multiwalled carbon nanotubes and gold nanoparticles. *Anal Methods* 2:837–843
 16. Zhang X, Duan S, Xu XM, Xu S, Zhou CL (2011) Electrochemical behavior and simultaneous determination of dihydroxybenzene isomers at a functionalized SBA-15 mesoporous silica modified carbon paste electrode. *Electrochim Acta* 56:1981–1987
 17. Shaikh AA, Saha SK, Bakshi PK, Hussain A, Ahammad AJS (2013) Poly(brilliant cresyl blue)-modified electrode for highly sensitive and simultaneous determination of hydroquinone and catechol. *J Electrochem Soc* 160:37–42
 18. Ahammad AJS, Rahman MM, Xu GR, Kim S, Lee JJ (2011) Highly sensitive and simultaneous determination of hydroquinone and catechol at poly(thionine) modified glassy carbon electrode. *Electrochim Acta* 56:5266–5271
 19. Vilian ATE, Chen SM, Huang LH, Ali MA, Al-Hemaid FMA (2014) Simultaneous determination of catechol and hydroquinone using a Pt/ZrO₂-RGO/GCE composite modified glassy carbon electrode. *Electrochim Acta* 125:503–509
 20. Guo HL, Peng S, Xu JH, Zhao YQ, Kang XF (2014) Highly stable pyridinic nitrogen doped graphene modified electrode in simultaneous determination of hydroquinone and catechol. *Sensors Actuators B Chem* 193:623–629
 21. Yue XY, Pang SP, Han PX, Zhang CJ, Wang JL, Zhang LX (2013) Carbon nanotubes/carbon paper composite electrode for sensitive detection of catechol in the presence of hydroquinone. *Electrochem Commun* 34:356–359
 22. Kumar A, Jena HM (2016) Preparation and characterization of high surface area activated carbon. *Results Phys* 6:651–658
 23. Bachrun S, AyuRizka N, Annisa SH, Arif H (2016) Preparation and characterization of activated carbon from sugarcane bagasse by physical activation with CO₂ gas. *IOP Conf Ser Mater Sci Eng* 105:12–27
 24. Jain A, Xu C, Jayaraman S, Balasubramanian R, Lee JY, Srinivasan MP (2015) Mesoporous activated carbons with enhanced porosity by optimal hydrothermal pre-treatment of biomass for supercapacitor applications. *Microporous Mesoporous Mater* 218:55–61
 25. Ghasemi M, Mashhadi S, Asif M, Tyagi I, Agarwal S, Gupta VK (2016) Microwave- assisted synthesis of tetraethylenepentamine functionalized activated carbon with high adsorption capacity for Malachite green dye. *J Mol Liq* 213:317–325
 26. Saeidi N, Parvini M, Niavarani Z (2015) High surface area and mesoporous graphene/activated carbon composite for adsorption of Pb(II) from wastewater. *J Environ Chem Eng* 3:2697–2706
 27. Zhu Z, Li A, Xia M, Wan J, Zhang Q (2008) Preparation and characterization of polymer based spherical activated carbons. *Chin J Polym Sci* 26:645–651
 28. Park JH, Park OO, Shin KH, Jin CS, Kim JH (2002) An electrochemical capacitor based on a Ni(OH)₂/activated carbon composite electrode. *Electrochem Solid State Lett* 5:7–10
 29. Stavropoulos GG, Zabanitout AA (2009) Minimizing activated carbons production cost. *Fuel Process Technol* 90:952–957
 30. Muniandy L, Adam F, Mohamed AR, Ng EP (2014) The synthesis and characterization of high purity mixed microporous/mesoporous activated carbon from rice husk using chemical activation with NaOH and KOH. *Microporous Mesoporous Mater* 197:316–323
 31. Malik R, Ramteke DS, Wate SR (2006) Physico-chemical and surface characterization of adsorbent prepared from groundnut shell by ZnCl₂ activation and its ability to adsorb colour. *Indian J Chem Technol* 13:319–328
 32. Gratuito MKB, Panyathanmaporn T, Chumnanklang RA, Sirintuntawittaya N, Dutt A (2008) Production of activated carbon from coconut shell: optimization using response surface methodology. *Bioresour Technol* 99:4887–4895
 33. Hussaro K (2014) Preparation of activated carbon from palm oil shell by chemical activation with Na₂CO₃ and ZnCl₂ as impregnated agents for H₂S adsorption. *Am J Environ Sci* 10:336–346
 34. Hammani H, Boumya W, Laghrib F, Farahi A, Lahrich S, Aboulkas A, El Mhammedi MA (2017) Electro-catalytic effect of Al₂O₃ supported onto activated carbon in oxidizing phenol at graphite electrode. *Mater Today Chem* 3:27–36
 35. Hammani H, Boumya W, Laghrib F, Farahi A, Lahrich S, Aboulkas A, El Mhammedi MA (2017) Electrocatalytic effect of NiO supported onto activated carbon in oxidizing phenol at graphite electrode: application in tap water and olive oil samples. *J Assoc Arab Univ Basic Appl Sci* 24:26–33
 36. Kumar K, Saxena RK, Kothari R, Suri DK, Kaushik NK, Bohra JN (1997) Correlation between adsorption and x-ray diffraction studies on viscose rayon based activated carbon cloth. *Carbon* 35:1842–1844
 37. Deraman M, Talib IA, Omar RM, Jumali HHJ, Taer E, Saman MM (2010) Microcrystallite dimension and total active surface area of carbon electrode from mixtures of PreCarbonized oil palm empty fruit bunches and green petroleum cokes. *Sains Malaysiana* 39:83–86
 38. Yang T, Lua A (2003) Characteristics of activated carbons prepared from pistachio-nut shells by physical activation. *J Colloid Interface Sci* 267:408–417
 39. Kuskur CM, Swamy BEK, Jayadevappa H (2017) Poly (naphthol green B) modified carbon paste electrode sensor for catechol and hydroquinone. *J Anal Chem* 804:99–106
 40. Ganesh PS, Swamy BEK (2016) Voltammetric resolution of catechol and hydroquinone at eosin Y film modified carbon paste electrode. *J Mol Liq* 220:208–215
 41. Naik TSSK, Swamy BEK (2017) Modification of carbon paste electrode by electrochemical polymerization of neutral red and its catalytic capability towards the simultaneous determination of catechol and hydroquinone: a voltammetric study. *J Anal Chem* 804:78–86
 42. Yin H, Ma Q, Zhou Y, Ai S, Zhu L (2010) Electrochemical behavior and voltammetric determination of 4-aminophenol based on

- graphene–chitosan composite film modified glassy carbon electrode. *Electrochim Acta* 55:7102–7108
43. Liu Z, Wang Z, Cao Y, Jing Y, Liu Y (2011) High sensitive simultaneous determination of hydroquinone and catechol based on graphene/BMIMPF 6 nanocomposite modified electrode. *Sensors Actuators B Chem* 157:540–546
 44. Song D, Xia J, Zhang F, Bi S, Xiang W, Wang Z, Xia L, Xia Y, Li Y, Xia L (2015) Multiwall carbon nanotubes-poly(diallyldimethylammonium chloride)-graphene hybrid composite film for simultaneous determination of catechol and hydroquinone. *Sensors Actuators B Chem* 206:111–118
 45. Gan T, Sun J, Huang K, Song L, Li Y (2013) A graphene oxide-mesoporous MnO₂ nanocomposite modified glassy carbon electrode as a novel and efficient voltammetric sensor for simultaneous determination of hydroquinone and catechol. *Sensors Actuators B Chem* 177:412–418
 46. Kumar M, Swamy BEK, Chandra U, Gebisa AW (2017) Co₃O₄/CuO composite nanopowder/sodium dodecyl sulphate modified carbon paste electrode based voltammetric sensors for detection of dopamine. *Int J Nanotechnol* 14:930–944
 47. Mohan K, Swamy BEK, Asif MHM, Viswanath CC (2017) Preparation of alanine and tyrosine functionalized graphene oxide nanoflakes and their modified carbon paste electrodes for the determination of dopamine. *Appl Surf Sci* 399:411–419
 48. Si WM, Lei W, Zhang YH, Xia MZ, Wang FY, Hao QL (2012) Electrodeposition of graphene oxide doped poly (3,4-ethylenedioxythiophene) film and its electrochemical sensing of catechol and hydroquinone. *Electrochim Acta* 85:295–301
 49. Shankar SS, Swamy BEK, Pandurangachar M, Chandra U, Chandrashekar BN, Manjunatha JG, Sherigara BS (2010) Electrocatalytic oxidation of dopamine on acrylamide modified carbon paste electrode: a voltammetric study. *Int J Electrochem Sci* 5:944–954
 50. Chandra U, Swamy BEK, Mahanthesha KR, Vishwanath CC, Sherigara BS (2013) Poly (malachite green) film based carbon paste electrode sensor for the voltammetric investigation of dopamine. *Chem Senses* 3:1–6
 51. Zheng LZ, Xiong LY, Li YD, Xu JP, Kang XW, Zou ZJ, Yang SM, Xia J (2013) Facile preparation of polydopamine-reduced graphene oxide nanocomposite and its electrochemical application in simultaneous determination of hydroquinone and catechol. *Sensors Actuators B Chem* 177:344–349
 52. Wang LP, Meng Y, Chen Q, Deng JH, Zhang YY, Li HT, Yao SZ (2013) Simultaneous electrochemical determination of dihydroxybenzene isomers based on the hydrophilic carbon nanoparticles and ferrocene-derivative mediator dual sensitized graphene composite. *Electrochim Acta* 92:216–225
 53. Wang L, Bai J, Wang H, Zhang L, Zhao Y (2007) Direct simultaneous electrochemical determination of hydroquinone and catechol at a poly(glutamic acid) modified glassy carbon electrode. *Int J Electrochem Sci* 2:123–132